Int. J. Electrochem. Sci., 10 **(2015)** 5942 - 5949

International Journal of
ELECTROCHEMICAL
SCIENCE
www.electrochemsci.org

Short Communication

Anatase TiO_2 Hollow Nanospheres with Ultrathin Shell Exhibit Superior Lithium Storage Property

Wei Zhou, Yourong Wang[*]*, Liping Zhang, Guangsen Song and Siqing Cheng*[*]

Innovation Center for Nanomaterials in Energy and Medicine (ICNEM), School of Chemical and Environmental Engineering, Wuhan Polytechnic University, Hubei 430023, P. R. China
[*]E-mail: icnem@hotmail.com

Received: 26 March 2015 / *Accepted:* 23 April 2015 / *Published:* 27 May 2015

TiO_2 hollow nanospheres with ultrathin shell of ca.10 nm were prepared by using sulfur nanospheres as templates and its electrochemical performance was investigated as anode material for lithium ion battery. The results show that the as-obtained anatase TiO_2 exhibits superior lithium storage capability due to its characteristic lithium storage mechanism and somewhat pseudocapacitive property. The as-obtained anatase TiO_2 electrode delivered a high initial specific capacity of 574.5 mAh g^{-1} at 168 mA g^{-1} and displays excellent cycling performance after first cycle, which might be attributed to the improvement of ionic and electron conduction of anatase TiO_2 due to the unique hollow nanostructure with ultrathin shell.

Keywords: Anatase TiO_2; Hollow nanospheres; Electrochemical performance; Anode materials; Lithium-ion battery.

1. INTRODUCTION

Nano-scale titanium dioxide (TiO_2), as one of the most versatile materials due to its intriguing properties, has been extensively investigated and applied in various fields such as photocatalysis, white pigments, dye-sensitized solar cells, biotechnology, cosmetics, energy storage, protective coating and others, which has been well documented in many reviews.[1–4] Recently, TiO_2 was considered as a promising anode material instead of conversional graphite[5] for the emerging large-sale lithium-ion batteries (LIBs) in stationary and automotive power storage application with a view to enhancing energy density, safety, power density, life, low temperature performance and quick-charge because compared to graphite,[6,7] (a) the safer lithium insertion/extraction potential of TiO_2 (1.5 – 1.8 V *vs.* Li^+/Li) prohibits the risk of metallic lithium deposition (Li-dendrite electroplating) and/or electrolyte

decomposition upon moderate overcharges and in normal operating conditions [2,8]; (b) considerable amounts of lithium could be reversibly inserted into TiO_2 within the electrochemical stability window of common organic electrolytes[9]; (c) the limited volume/structure variation (less than 4%) during the Li^+ insertion/extraction process results in a prolonged cycling life due to an enhanced structural stability[10,11]. Beside these, TiO_2 offers several other advantages as being environmentally friendly, abundant and inexpensive.[12] However, the low ionic and electrical conductivity of TiO_2 which will cause limited specific capacity and poor cycling performance have seriously hampered its practical electrochemical performance.[13,14] To solve these problems, vast approaches have been developed by modifying structure and composition of pure TiO_2. Among them nanosized TiO_2 particles have been demonstrated to shorten the diffusion lengths for electrons and Li^+ ions and thus leading to improved results in terms of high rate capability, rate and cycling stabilities as well as higher capacities.[2,15–17] In particular, nanometer-sized particles with a one-dimensional (1D) structure, such as nanotubes[18], nanorods[19], and nanowires[20], have attracted great interest due to easy Li^+ ion diffusion into the TiO_2 host structure caused by their high specific surface area and low particle size. Unfortunately, poor electronic conduction network due to severe aggregation of nanoparticles, loss of particle connection during the charge-discharge process and low packing density impose another challenge in practical applications.[21] Recently, it has been proposed that TiO_2 hollow structures consisting of nanosized building blocks could partly overcome these shortcomings while retaining high electrochemical activity.[3,6,19,22,23] The properties of hollow materials endow high contact area between electrolyte and electrode and good accommodation of strain during cycling, thus facilitating ion diffusion and electron transfer in electrochemical reactions. However, most TiO_2 hollow structures reported in the literature exhibit unsatisfactory cycling stability and discharge specific capacity, which is perhaps as a result of the relatively large size and shell thickness of hollow particles consisting of nanosized building blocks. It is thus very important to develop simple strategies for engineering a novel hollow nanostructured TiO_2 with ultrathin wall.

In this paper, we report a simple and low-cost template-assisted method to construct a novel hollow nanostructured TiO_2 with ultrathin wall. Sulfur spheres are used as the soft template. The electrochemical performance of the as-prepared TiO_2 anode in LIBs, especially for lithium storage property was evaluated.

2. EXPERIMENTAL SECTION

2.1 Material synthesis.

All reagents were of analytical pure from the commercial market and used as received without further purification. First, sulphur nanoparticles as templates were synthesized by adding quickly 4 ml of 36.5 wt% concentrated HCl to a 500 ml of 0.063 M $Na_2S_2O_3$ aqueous solution containing 0.1024 g of polyvinylpyrrolidone (PVP, Mw ~ 55,000). After reaction for 4 h, the as-prepared sulphur nanoparticles were washed three times with deionized water by ultrasonication and centrifugation (3500 r/min), and redispersed into a 100 ml of 0.01 wt% PVP aqueous solution by ultrasonication for 5

min. The resulting solution of sulphur nanoparticles was mixed with 400 ml of isopropanol and 10 ml of 28 wt% concentrated ammonia under magnetic stirring. 250 ml of 0.01 M tetrabutyl titanate in isopropanol was then added in five portions (5 × 50 ml) at half hour intervals. After reaction of 4 h, the solution of sulphur-TiO_2 core-shell nanoparticles was washed three times with deionized water and ethanol, respectively, by centrifugation and ultrasonication to remove freely hydrolysed TiO_2, and dried under vacuum overnight. Hollow TiO_2 nanostructures were obtained by annealing the sulphur-TiO_2 core-shell nanoparticles in a muffle furnace equipped with programmed temperature at 300 ^{0}C in air for 30 min.

2.2 Material characterization.

Powder X-ray diffraction (XRD, DX-6000, Shimadzu) patterns were collected on a diffractometer with Cu Kα radiation with λ = 1.5418 Å at a scanning step of 2° per minute between 10° and 80°. Nitrogen adsorption-desorption isotherms and the Brunauer-Emmett-Teller (BET) method were analyzed using a TriStar surface area&porosity analyzer at 77 K. Field emission scanning electron microscope (FESEM) images were taken by a Hitachi SEM. The samples were prepared by sonicating the products in absolute ethanol and evaporating one drop of suspension on conductive adhesive. The transmission electron microscopy (TEM) and high-resolution transmission electron microscopy (HRTEM) images were acquired using a JEOL JEM-2010 HRTEM operating with an acceleration voltage of 200 kV. The samples were prepared by dipping an amorphous carbon-copper grid in a dilute solution of samples dispersed in absolute ethanol.

2.3 Electrochemical evaluation.

The electrochemical experimental methods were similar to the ones in our previous study. The preparation of working electrodes were as followed: A slurry consisting of 70 wt% of hollow nanosized TiO_2, acetylene black (20 wt%), and polyvinylidene fluoride (PVDF, 10 wt%) in N-methyl-2-pyrrolidone (NMP) was uniformly coated on a piece of foil. The active material loading was 1-2 mg/cm^2. Then, the Cu foil coated with the mixture was dried at 80^{0}C overnight. Finally, the TiO_2 electrodes were assembled into coin-type 2016 cell. Metallic lithium was used as the anode and liquid mixtures containing 1 mol L^{-1} $LiPF_6$ and a solvent mixture of ethylene carbonate and dimethyl carbonate (1 : 1, v/v)were used as electrolyte.The assembled cells were tested at room temperature by a program-controlled Battery Test System (Land®, Wuhan, China) for the electrochemical performance and by using a CHI660B electrochemical workstation (Chenghua, Shanghai, China) for the cyclic voltammetry (CV).

3. RESULTS AND DISCUSSION

The hollow structures are generally designed controllably by deposition on diverse removable hard templates such as polymers, silica, and other colloid particles, followed by selective removal of the templates via chemical etching or thermal decomposition[24,25], which has been considered to be

one of the most versatile and straightforward strategies towards hollow structures. The uniformity and the wall thickness of hollow structures are strongly dependent on the used template. Herein, sulphur nanospheres was employed as template to fabricate the TiO_2 hollow nanostructures, which is seldom reported before, given that uniform sulphur nanospheres are apt to be tuned by using the surfactant PVP and to be removable by annealing in air, which produces a highly crystalline TiO_2 products.

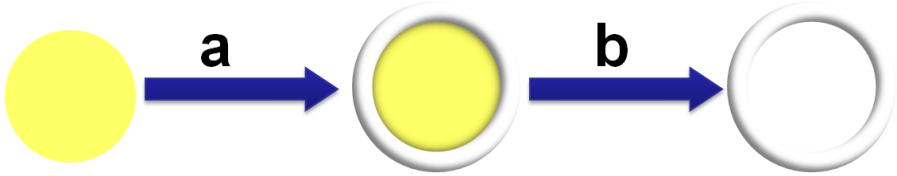

Figure 1. Schematics of the preparation of anatase TiO_2 hollow nanosphere with ultrathin shell. (a) the deposition of TiO_2 (white) on sulfur nanosphere (yellow); (b) calcination of S/TiO_2 core-shell composite to form TiO_2 hollow nanosphere with ultrathin shell.

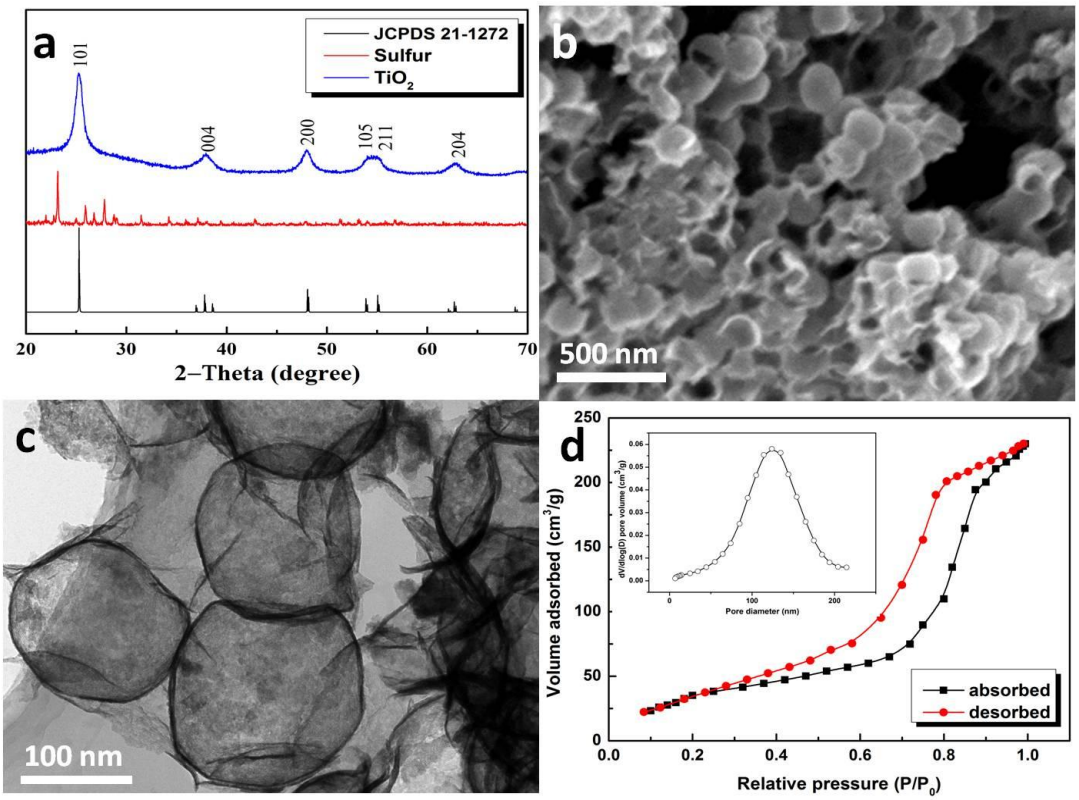

Figure 2. (a) Powder X-ray diffraction patterns of sulfur, the as-obtained TiO_2 and standard anatase TiO_2; (b) SEM image of the as-obtained TiO_2; (c) TEM image of the as-obtained TiO_2; (d) Nitrogen adsorption-desorption isotherm (inset: pore size distribution) of the obtained anatase TiO_2 hollow nanosphere with ultrathin shell. phase (JCPDS card no. 21-1272).

Meanwhile, sulphur nanospheres are liable to be dispersed in solvents, which is favorable to uniform deposition TiO_2 layer. In our experiments, the concentration of PVP was controlled to be very low (0.01 wt%) because it was found that the obtained sulphur nanospheres are hollow in the presence

of high concentration of PVP (not shown here), which is detrimental to support TiO_2 coating. Thus, the synthesis of TiO_2 hollow nanospheres is simple and straightforward, as illustrated in Fig.1.

The morphological and structural characterizations of the as-obtained TiO_2 hollow nanostructures are shown in Fig. 2. The phase purity of the annealed sample is examined by powder X-ray diffraction (XRD) analysis (Fig.2a), where the diffraction pattern with typical location at $\theta = 27.4°$ can be readily indexed to the anatase TiO_2

Compared to the diffraction pattern of sulfur, it is indicative of the formation of pure anatase TiO_2 phase without any sulfur residues. In addition, the wider and weaker diffraction peaks of the sample suggest the prepared anatase TiO_2 are constructed with nanosized particles. According the Debye-Scherrer formula, the average diameter of particle is calculated to be approximately 9.2 nm from the most intense peak (101). The morphology is presented clearly by SEM image (Fig. 2b) and the diameter of these TiO_2 hollow nanospheres is in the range of 100 to 200 nm, indicating the perfectly retained spherical morphology after thermal annealing treatment. The hollow center of the annealed product is clearly shown via the TEM image (Fig. 2c), in which a spherical interior with a distinct contrast difference to shell is evident. The shell of TiO_2 hollow nanosphere is evaluated to be ca. 10 nm in thickness, which is roughly consistent with XRD result. This might be because the release of gaseous species from combustion of sulfur spheres inhibits the growth of TiO_2 crystallites so that thin TiO_2 shell is generated. Nitrogen isothermal adsorption-desorption measurements were performed to determine the Brunauer-Emmett-Teller (BET) specific surface area and the porosity of the as-obtained antatase TiO_2, as shown in Fig.2d for the isotherm curve. It can be seen that the isotherm curve is a typical Type IV isotherm representing nanoporous structure with a BET specific surface area of 125 $m^2 g^{-1}$ and the pore size distribution shown in Figure 2d inset displays a unimodal peak around 124 nm. As such, the high specific surface area and the hollow nanostructure with ultrathin shell of the as-obtained anatase TiO_2 should give rise to significant improvement in the specific discharge capacity and rate capability of TiO_2 anode for LIBs.

For anatase TiO_2, it appears more facile for the uptake of Li^+ due to its planar double chains lattice structure with a tetragonal body-centered space group $I4_1/amd$ consisting of TiO_6 octahedra, compared to other polymorphs of TiO_2[26], suggesting the unique lithium insertion and extraction mechanism of anatase TiO_2. The electrochemical properties of lithium insertion and extraction for the as-obtained TiO_2 electrode have been performed by cyclic voltammetry (CV) and galvanostatic charge (lithium insertion)-discharge (lithium extraction) tests. Fig. 3a shows the first three cyclic voltammograms of TiO_2 electrode at a scan rate of 0.2 mV s^{-1} in the potential window of 1.00 -3.00 V. The characteristic couple of cathodic and anodic peaks in the CV at ~ 1.65 V and ~ 2.0 V are observed, respectively, versus Li^+/Li, corresponding to the Li^+ insertion/re-insertion processes into the anatase TiO_2 host structure, which is consistent with previously reported values[27], representing the classical two phase electrochemical reaction process of the Li-insertion/extraction with the Li-poor $Li_{0.01}TiO_2$ phase and the Li-rich $Li_{0.55}$ TiO_2 phase. Notably, the weak new peak couple appears at 1.45 V and 1.75 V, respectively for the lithium insertion/extraction process, as marked by arrow in Fig. 3a, indicating the further transformation of the formed $Li_{0.55}TiO_2$ phase to a new occurring phase ($LiTiO_2$)[10], which ascribes to the nanosized particles.

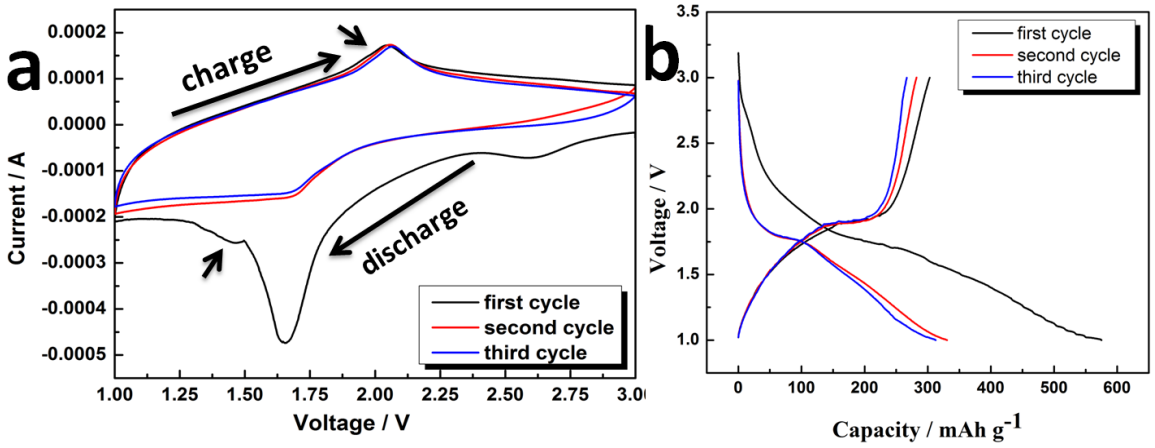

Figure 3. (a) The first three cycles cyclic voltammograms of the obtained anatased TiO_2 electrode at a scan rate of 0.2 mV s^{-1} in the potential window of 1.00 -3.00 V; (b) the galvanostatic charge-discharge voltage profiles of the as-obtained anatase TiO_2 electrodes with a cut-off voltage window of 1.0 – 3.0 V versus Li^+/Li for the first three cycles at the discharge current density of 168 mA g^{-1}.

In addition, the cathodic peak sharply decreases after the first cycle with cycling and the CV curves with characteristic pseudocapacitive behavior in the following cycles almost overlap. This might be contributed by the irreversible extensive decomposition of electrolyte accompanying the formation of the solid-electrolyte interface (SEI) due to the large surface area of the hollow nanosized structure with ultrathin wall after the first-cycle discharge.[28] The overlapped following cycles indicate a potential rate capability. All these are demonstrated further in the charge-discharge curves, as shown in Fig. 3b for the galvanostatic charge-discharge voltage profiles of the as-obtained anatase TiO_2 electrodes with a cut-off voltage window of 1.0 – 3.0 V versus Li^+/Li for the first three cycles at the discharge current density of 168 mA g^{-1}. There are two appreciable voltage plateaus in the charge-discharge curves at approximately 1.75 V and 1.9 V versus Li^+/Li, respectively, which is related to the lithium insertion/extraction process. The as-obtained anatase TiO_2 delivers a pretty high initial discharge specific capacity of 574.5 mA h g^{-1}, which is much more high than the theoretical specific capacity of anatase TiO_2 of 375 mA h g^{-1}. This might be contributed to the formation of SEI, as evidenced by CV above. More importantly, the second cycle and the third cycle give rise to the close reversible capacity of 329 mAh g^{-1} and 315 mAh g^{-1}, respectively, which is equivalent to be 88% and 84% of the theoretical specific capacity of anatase TiO_2, representing the good capacity retention. It is believed that this should be attributed to the unique hollow structure with ultrafine shell of TiO_2. On one hand, the hollow structure with ultrathin shell makes TiO_2 to contact with conducting assistant material sufficiently, resulting in the electronic conductivity improved, hence improving the specific capacity. On the other hand, the unique structure also makes most of TiO_2 contact with electrolyte, reducing the Li^+ diffusion distance, thus improving the cycling performance. Meanwhile, the hollow TiO_2 with large area could also provide some extra site occupations for lithium insertion, which may also contribute to the specific capacity.

4. CONCLUSIONS

In summary, anatase TiO_2 hollow nanospheres with ultrathin shell of ca. 10 nm were prepared successfully by using sulfur nanospheres as templates, and the BET specific area and the pore size were determined to be 125 m^2 g^{-1} and 124 nm, respectively, which was reported rarely before. The as-obtained anatase TiO_2 as anode material for lithium-ion battery represents the classic bi-phase process of lithium storage while the much more lithium storage occurs to form a new phase due to its hollow nanospherical structure, as evidenced by CV curves, indicating the superior lithium storage. In addition, the as-obtained anatase TiO_2 also exhibits somewhat pseudocapacitive property to some extent with cycling, which might contribute to the specific capacity of the obtained sample. Thus, the as-obtained anatase TiO_2 electrode delivers an initial specific capacity of 574.5 mAh g^{-1} at a current density of 168 mA g^{-1} and presents the excellent cycling performance in subsequent cyclings with no appreciable change in capacity, representing the improved greatly electrochemical performance. All these are attributed to the unique hollow nanosized structure with ultrathin shell because this allows the sufficient contact of TiO_2 with electrolyte and conductive assistant material, reducing Li^+ diffusion path and increasing the electron conduction of TiO_2. Therefore, we believe that this unique structure of anatase TiO_2 is potential for exploring the anatase TiO_2 as anode material for lithium ion battery in the future. Further detailed investigations including the rate capability and high rate performance are underway in our laboratory.

ACKNOWLEDGEMENTS
This work is supported by Hubei Provincial Natural Science Foundation of China (No. 2015CFC842), Education Foundation of Hubei Province (No. T200908), Project of Chinese Ministry of Education (No. 208088).

References

1. G.-N. Zhu, Y.-G. Wang and Y.-Y. Xia, *Energy Environ. Sci.*, 5 (2012) 6652.
2. Z. Yang, D. Choi, S. Kerisit, K.M. Rosso, D. Wang and J. Zhang, *J. Power Sources*,192 (2009) 588.
3. W. Wei, Z. Wang, Z. Liu, Y. Liu, L. He and D. Chen, *J. Power Sources*, 238 (2013) 376.
4. X. Chen and S.S. Mao, *Chem. Rev.*, 107 (2007) 2891.
5. M. Endo, C. Kim, K. Nishimura, T. Fujino and K. Miyashita, *Carbon*, 38 (2000) 183.
6. Z. Wang, L. Zhou and X. W. Lou, *Adv. Mater.*, 24 (2012) 1903.
7. L. Ji, Z. Lin, M. Alcoutlabi and X. Zhang, *Energy Environ. Sci.*, 4 (2011) 2682.
8. B. Scrosati and J. Garche, *J. Power Sources*, 195 (2010) 2419.
9. H. Wang, J. He, G. Boschloo, H. Lindström, A. Hagfeldt and S.-E. Lindquist, *J. Phys. Chem. B.*, 105 (2001) 2529.
10. M. Wagemaker, G.J. Kearley, A.A. van Well, H. Mutka and F.M. Mulder, J. Am. Chem. Soc., 125 (2003) 840.
11. V. G. Pol, S.-H. Kang, J. M. Calderon-Moreno, C. S. Johnson and M. M. Thackeray, *J. Power Sources*, 195 (2010) 5039.
12. D. Deng, M.G. Kim, J.Y. Lee and J. Cho, *Energy Environ. Sci.*, 2 (2009) 818.
13. S. Yoon, B. H. Ka, C. Lee, M. Park and S. M. Oh, *Electrochem. Solid-State Lett.*, 12 (2009) A28.

14. F. Gligor and S. Deleeuw, *Solid State Ion*, 177 (2006) 2741.
15. V. Subramanian, A. Karki, K. I. Gnanasekar, F. P. Eddy and B. Rambabu, *J. Power Sources*, 159 (2006) 186.
16. G. Qin, H. Zhang and C. Wang, *J. Power Sources*, 272 (2014) 491.
17. S. Moitzheim, C. S. Nimisha, S. Deng, D. J. Cott, C. Detavernier and P. M. Vereecken, *Nanotechnology*, 25 (2014) 504008.
18. J. Xu, C. Jia, B. Cao and W. F. Zhang, *Electrochimica Acta*, 52 (2007) 8044.
19. S.-J. Bao, Q.-L. Bao, C.-M. Li and Z. L. Dong, *Electrochem. Commun.*, 9 (2007) 1233.
20. Y. Wang, M. Wu and W.F. Zhang, *Electrochimica Acta*, 53 (2008) 7863.
21. X. Su, Q. Wu, X. Zhan, J. Wu, S. Wei and Z. Guo, *J. Mater. Sci.*, 47 (2012) 2519.
22. W. Wang, F.-X. Bu and J.-S. Jiang, *Mater. Lett.*, 139 (2015) 89.
23. H. Liu, Z. Bi, X.-G. Sun, R. R. Unocic, M. P. Paranthaman and S. Dai, *Adv. Mater.*, 23 (2011) 3450.
24. J. Hu, M. Chen, X. Fang and L. Wu, *Chem. Soc. Rev.*, 40 (2011) 5472.
25. X. Lai, J. E. Halpert and D. Wang, *Energy Environ. Sci.*, 5 (2012) 5604.
26. M. Wagemaker, *Solid State Ion*, 175 (2004) 191.
27. D. Bresser, E. Paillard, E. Binetti, S. Krueger, M. Striccoli and M. Winter, *J. Power Sources*, 206 (2012) 301.
28. C. Jiang, M. Wei, Z. Qi, T. Kudo, I. Honma and H. Zhou, *J. Power Sources*, 166 (2007) 239.